Exp.-Nr.: A1/2–00
Eingang: 20.12.00
an PAC:

Mainz Microtron MAMI

Collaboration A1: "Virtual Photons"

Spokesperson: R. Neuhausen

Proposal for an Experiment

The Structure of ^{3}He

Collaborators:

F.Bloch, C.Carasco, M.Hauger, J.Jourdan, T.Klechneva, B.Krusche, K.Normand, D.Rohe*, I.Sick, G. Warren, H.Wöhrle
(Institut für Physik, Universität Basel)

J. Golak, W. Glöckle, H. Kamada, H. Witała
(Institut für Theoretische Physik II, Ruhr-Universität Bochum and Institute of Physics, Jagellonian University Cracow)

M. Potokar, S. Širca
Institut "Jožef Stefan", Univ. of Ljubljana, Slovenia

J. Bermuth, W.Heil*, E.W.Otten
(Institut für Physik, Universität Mainz)

P. Bartsch, D. Baumann, R. Böhm, M. Ding, M.O. Distler*, S. Derber, D. Elsner, J. Friedrich, S. Hedicke, P. Jennewein, F. Klein, K.W. Krygier, H. Merkel, K. Merle, P. Merle, U. Müller, R. Neuhausen, M. Seimetz, H. Schmieden, A. Süle, Th. Walcher, M. Weis
(Institut für Kernphysik, Universität Mainz)

P. Grabmayr
(Institut für Physik, Universität Tübingen)

*Contact Person

Exp.-Nr.: A1/2–00

Eingang: 20.12.00

Mainz Microtron MAMI

Collaboration: A1

Spokesperson: R. Neuhausen

Title: The Structure of ^{3}He.

Authors: P. Bartsch[1], D. Baumann[1], J. Bermuth[2], F. Bloch[3], R. Böhm[1], C. Carasco[3], M. Ding[1], M.O. Distler[1], S. Derber[1], D. Elsner[1], J. Friedrich[1], W. Glöckle[4], J. Golak[4], P. Grabmayr[5], M. Hauger[3], S. Hedicke[1], W. Heil[2], P. Jennewein[1], J. Jourdan[3], H. Kamada[4], T. Klechneva[3], F. Klein[1], B. Krusche[2], K.W. Krygier[1], H. Merkel[1], K. Merle[1], P. Merle[1], U. Müller[1], R. Neuhausen[1], K. Normand[3], E.W. Otten[2], M. Potokar[6], D. Rohe[3], H. Schmieden[1], M. Seimetz[1], I. Sick[3], S. Širca[6], A. Süle[1], Th. Walcher[1], G. Warren[3], M. Weis[1], H. Witała[4], H. Wöhrle[3]

[1]*Institut für Kernphysik, Universität Mainz,* [2]*Institut für Physik, Universität Mainz,* [3]*Institut für Physik, Universität Basel,* [4]*Institut für Theoretische Physik II, Ruhr-Universität Bochum and Institute of Physics, Jagellonian University Cracow,* [5]*Institut für Physik, Universität Tübingen,* [6]*Institut "Jožef Stefan", Univ. of Ljubljana, Slovenia*

Contactperson: M.O. Distler, W. Heil and D. Rohe

Abstract of physics: We propose to study the nuclear structure of ^{3}He and the reaction mechanism of $^3\mathrm{He}(\mathrm{e},\mathrm{e'N})$ via measurements of the asymmetries in $^3\vec{\mathrm{He}}(\vec{\mathrm{e}},\mathrm{e'p})$ and $^3\vec{\mathrm{He}}(\vec{\mathrm{e}},\mathrm{e'n})$–scattering.

Abstract of equipment: The experiment will employ the $^3\vec{\mathrm{He}}$–target developed at the University of Mainz. Spectrometer A will detect the scattered electron in coincidence with the recoiling particles detected with two special nucleon detectors and spectrometer B. The beam polarization will be measured with the Møller polarimeter.

MAMI-Specifications :

beam energy:	min.	790 MeV	max.	855 MeV
beam current:	min.	5.0 μA	max.	15.0 μA
time structure:	continuous beam			
polarization:	yes			

Experiment-Specifications :

hall: spectrometer hall

beam line: standard to spectrometer hall

spectrometer:	particles:	range of angles:	out of plane:
A	e^-	48.1^o	-
B	p	50.5^o	-

special detectors: Two segmented BC400 scintillator telescopes. Angular range 24^o-40^o and 60^o-76^o.

targets and chamber : $^3\vec{\mathrm{He}}$–cell with magnetic holding field and shielding box

Beam time request :

set-up without beam:	400 h
set-up with beam:	80 h
data taking:	520 h

1 Motivation

Investigations of the structure of the nuclear three–body system have recently attracted a lot of interest. One of the driving forces for this interest are modern three-body calculations which allow for a quantitative description of the three-nucleon system not only of the ground state but also for the continuum states. These calculations have reached a high degree of sophistication, and several "exact" calculations are available today [1, 2]. The calculations are generally done in a non-relativistic framework, and provide solutions of the Schrödinger equation in configuration or momentum space for three structureless nucleons interacting via one of the standard nucleon-nucleon potentials. This progress opens the possibility to test our understanding of the three-body system not only via ground state observables but also by using the continuum observables, quantities that obviously have a much richer structure and contain additional information.

For the three-body ground state, the calculations predict a number of different wave function components with total angular momentum of $L = 0, 2$, the total probability of the $L \neq 0$ states amounting to 6÷9% [3]. A number of experimental observables have been used to check the predictions of these calculations. We mention in particular elastic electron scattering [4], $(e, e'p)$–reaction [5–7], and nucleon-deuteron scattering [8]. The comparisons show that the calculations are quite successful. However, in these processes the $L \neq 0$ states in general give only small effects, in accordance with the small probability of the corresponding wave function components. On the other hand, the three–body calculations fail to reproduce the triton binding energy and it is presently not understood to what extend the strength of the $^3S_1$–$^3D_1$ tensor force (which leads to the $L \neq 0$–wave function components) or an additional three-nucleon force is responsible for the discrepancy. Thus, for a quantitative understanding of the A=3 systems, these small wave function components are very crucial, and need to be experimentally investigated.

In addition, the understanding of $L \neq 0$ states is particularly important if one is interested in processes sensitive to non-nucleonic degrees of freedom. Processes involving pions or deltas often involve transitions with $\Delta L \neq 0$, given the p-wave coupling of the pion to the nucleon, and the spin of 3/2 of the delta. In the A=3 magnetic form factor, for instance, the nucleonic ΔL=2 transition and meson exchange currents (MEC) give large, but essentially opposite, effects; a similar observation applies to deuteron electro-disintegration [9]. For a better understanding of the non-nucleonic degrees of freedom it is clearly imperative to have a good control over the $L \neq 0$ components of the wave function.

Compared to the cross section observables mentioned above, polarization observables are preferred for the study of $L \neq 0$–wave function components. The S–S amplitude, which usually dominates unpolarized cross sections, is strongly suppressed in these observables which thus allows for a study of the small S–D–amplitudes. With the present proposal we aim at a study of these $L \neq 0$ components in the ^{3}He–ground state wave function via a measurement of spin observables of the $^3\vec{\mathrm{He}}(\vec{e}, e'p)$ and $^3\vec{\mathrm{He}}(\vec{e}, e'n)$–reactions.

The measurement of polarization observables in the radiative capture reaction ^{1}H($\vec{d}$,γ)^{3}He provides one way to study small wave function components and non–nucleonic degrees of freedom in the ^{3}He–system. This technique is being pursued by the Basel group since several years at the Philips injector at PSI [10, 11]. In the energy range of the capture reaction experiment (30–45 MeV) the dominant contribution to the reaction amplitude is an electric dipole transition (E1). Contributions of non–nucleonic degrees of freedom are implicitly included in calculations of the reaction amplitude due to the Siegert theorem. A measurement of the tensor analyzing power A_{yy} at medium scattering angles, where E1 dominates, provides a measure of some components of the $L = 2$ contribution to the ^{3}He–ground state. This sensitivity to the D–state contributions has been confirmed with the recent Faddeev calculations [11].

The sensitivity of the capture reaction to the various components that contribute to the D–state of ^{3}He has been discussed long ago in a paper by Ericson and Iudice [12]. They conclude that the dominant contribution to A_{yy} results from the $l = \lambda = 1$ component of the D–state with l the relative angular momentum of the 'interacting' pair and λ the angular momentum of the third particle relative to the center of mass of the interacting pair. The same paper suggests that the dominant contribution to the D–state with $l = 2, \lambda = 0$ can not be investigated in these experiments, but that the asymmetries in $^3\vec{\mathrm{He}}(\vec{\mathrm{e}}, \mathrm{e}'\mathrm{p})$ and $^3\vec{\mathrm{He}}(\vec{\mathrm{e}}, \mathrm{e}'\mathrm{n})$–scattering are sensitive to it [13].

The study of few–body systems in general and ^{3}He in particular is also important from a more fundamental point of view. The investigation of the properties of the ground state and excited states of the nucleon offers the most direct way for tests of the fundamental theory of strong interactions - quantumchromodynamics (QCD) - in the non-perturbative low energy regime. During the last few years, predictions for nucleon ground state properties directly derived from QCD via lattice gauge calculations became available (see e.g. [14]) and great progress was made in the development of effective field theories like chiral dynamics (see e.g. [15]) based on the fundamental symmetries of QCD. Consequently, considerable and ongoing efforts have been put into scattering experiments and photo-, electro-, and hadron production experiments of mesons from nucleons at accelerator facilities like MAMI (Mainz), ELSA (Bonn), Bates (MIT), JLab (Newport News), COSY (Jülich), and PSI (Villingen).

Detailed tests of the theoretical concepts require measurements not only of the proton but also of the neutron properties. However, due to the nonavailability of free neutron targets, only neutrons bound in light nuclei can be studied. The most important target nuclei for this purpose are the deuteron and ^{3}He. The deuteron is singled out due to the low binding energy and the comparatively well understood nuclear structure. The main advantage of ^{3}He lies in the fact that for the major contributions of the ground state wave function the spins of the two protons are coupled antiparallel so that spin dependent effects are dominated by the neutron.

In principle, it is possible to extract information about neutron properties like form factors or meson production cross sections from an inclusive measurement from light nuclei. However, experiments where physical quantities are little affected by nuclear effects are limited to very few special cases. An example is η-photoproduction in the second resonance region where the results derived from inclusive [16] and exclusive measurements from different target nuclei [17,18] are in very good agreement. On the other hand, a precise extraction of the neutron magnetic form factor, G_{mn}, requires a detailed understanding of nuclear effects. Only a spin–dependent quasi–elastic experiment on $^3\vec{\mathrm{He}}$ with a careful treatment of reaction dynamics corrections allows to successfully determine G_{mn} [19].

Thus, for most of the interesting physical quantities it is necessary to perform an *exclusive* measurement in which the struck particle is detected and the reaction channel is identified. In addition, nuclear structure effects such as final state interactions (FSI), and meson exchange currents (MEC), must be carefully considered. One of the best examples are recent determinations of the neutron electric form factor, G_{en}, extracted from spin–dependent measurements on the deuteron and ^{3}He [20–25]. A comparison of the results has shown that the consistency of the data from the different target nuclei without the application of substantial corrections for nuclear structure effects and FSI is unsatisfactory. For studies using ^{3}He as a target the recent results by Poolman underlies the importance of FSI–effects as a basic component of three–body–calculations [26].

Besides the elastic form factors of the neutron, the study of the Gerasimov–Drell–Hearn sum rule (GDH) and the Q^2–evolution of the extended GDH sum rule are in progress or planned at MAMI and JLab [27, 28]. The extraction of fundamental information for the neutron from spin–dependent observables with $^3\vec{\mathrm{He}}$–targets also requires a quantitative correction of nuclear structure effects [29, 30].

Whereas the calculations of such corrections for the deuteron have been carefully tested in many experiments, a detailed experimental study of the nuclear structure and FSI effects for ^{3}He is not at hand. Thus, with the present proposal we do not only want to study the nuclear structure of ^{3}He but also to test the reliability of the calculations in view of nuclear structure corrections in general and FSI effects in particular.

2 Status of Research

2.1 Theory

An approach suitable to test the D–state component with $l = 2, \lambda = 0$ was first suggested by Blankleider and Woloshyn [13]. They performed an impulse approximation calculation for spin–dependent quasi–elastic electron scattering on ^{3}He with polarized electrons and target. They found that the asymmetry in the wings of the quasi–elastic peak from the proton contribution is mainly coming from the small wave function components, dominantly the $l = 2, \lambda = 0$–channel, of the D–state. Thus, as suggested by Ericson et al. asymmetry measurements in the $^3\vec{\mathrm{He}}(\vec{\mathrm{e}}, \mathrm{e}'\mathrm{p})$ and $^3\vec{\mathrm{He}}(\vec{\mathrm{e}}, \mathrm{e}'\mathrm{n})$ reactions could provide a sensitive test of this component.

A calculation of the spin dependent structure functions for the ^{3}He–ground state has been performed by Schulze and Sauer [31] within a Faddeev approach. The results of this calculation show that for low Fermi momenta (top of the quasi–elastic peak) the neutron has its spin completely parallel to the nuclear spin; however at high Fermi momenta (wings of the quasi–elastic peak), the D-state is sizeable as the neutron spin can be found with high probability *opposite* to the nuclear spin. Thus, these studies confirm the original calculations by Blankleider and Woloshyn.

The rigorous Faddeev approach by Golak *et al.* [32] for ground and continuum states allows to study weather these findings hold in the presence of FSI and MEC effects. In order to support the present proposal, several predictive calculations of the asymmetries for $^3\vec{\mathrm{He}}(\vec{\mathrm{e}},\mathrm{e}'\mathrm{n})$ and $^3\vec{\mathrm{He}}(\vec{\mathrm{e}},\mathrm{e}'\mathrm{p})$ have been performed [33].

These calculations are done for an incident electron energy of 790 MeV, electron scattering angle of 48.1^o, and three different energy loss values of the scattered electron in the range of the quasi–elastic peak ($\omega = 175, 128, 98$ MeV). The kinematic conditions are qualitatively illustrated in figure 1, which is an experimental spectrum taken at a similar kinematics [34]. The energy loss values of the calculations scaled to the different kinematics are indicated with labeled arrows (K1,K2, and K3). Scaling is performed for constant y–scaling values [35].

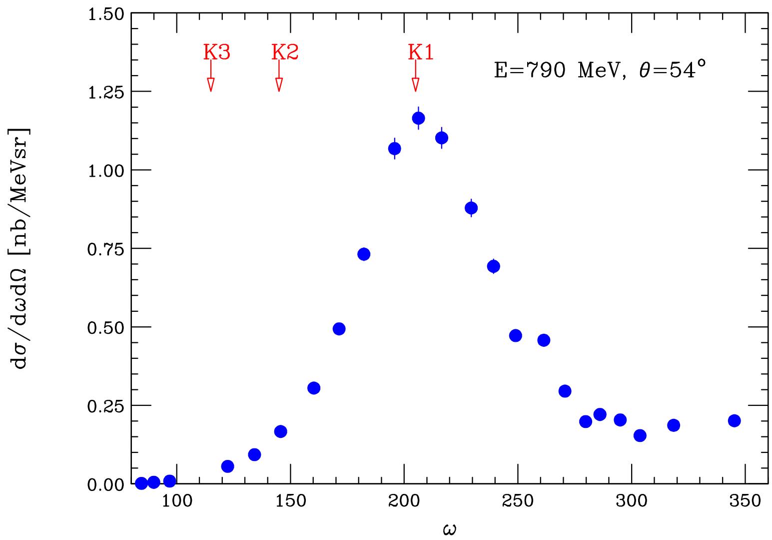

Figure 1: An experimental spectrum of $^3\mathrm{He}(e,e')$ measured at Bates [34] at a kinematics similar to the one of the present proposal. Indicated with labeled arrows are the energy loss values for which the $^3\vec{\mathrm{He}}(\vec{\mathrm{e}},\mathrm{e}'\mathrm{n})$ and $^3\vec{\mathrm{He}}(\vec{\mathrm{e}},\mathrm{e}'\mathrm{p})$ calculations have been performed.

For the three kinematical conditions the expression

$$\frac{d\sigma}{d\Omega_e d\omega d\Omega_i dE_m} = \Sigma(\theta^*,\phi^*) + h\Delta(\theta^*,\phi^*)$$

is calculated with $i = p$ for $^3\vec{\mathrm{He}}(\vec{\mathrm{e}},\mathrm{e}'\mathrm{p})$ and $i = n$ for $^3\vec{\mathrm{He}}(\vec{\mathrm{e}},\mathrm{e}'\mathrm{n})$ [36]. E_m is the energy of the remaining two–nucleon system usually denoted as the missing energy. The cross section is written as a sum of a helicity independent part, Σ, and a part Δ that depends on the helicity h of the electron beam. Both parts depend on the direction of the target spin defined by the angles θ^* and ϕ^* with respect to the direction of the momentum transfer $\vec{q}$. The asymmetries parallel to $\vec{q}$, A_z, and perpendicular to $\vec{q}$, A_x, discussed in the following are defined as:

$$A_z = \frac{\Delta(0^o, 0^o)}{\Sigma(0^o, 0^o)} \qquad \text{and} \qquad A_x = \frac{\Delta(90^o, 0^o)}{\Sigma(90^o, 0^o)}.$$

For the $^3\vec{\mathrm{He}}(\vec{\mathrm{e}}, \mathrm{e}'\mathrm{p})$–reaction the two–body breakup channel (2BB) as well as the three–body breakup channel (3BB) have been calculated. The latter for a grid of E_m–values in the range from threshold to 24.7 MeV. In agreement with the experimental results by Florizone *et al.* [6, 7] most of the strength of the 3BB is concentrated close to the threshold with a rapid fall–off of the strength as a function of E_m. In figure 2 the calculated cross section for several E_m of $^3\vec{\mathrm{He}}(\vec{\mathrm{e}}, \mathrm{e}'\mathrm{p})$ as a function of the scattering angle of the knocked–out proton is shown. Considering the logarithmic scale of the figure, the calculation predicts also a very fast fall–off for the present kinematics.

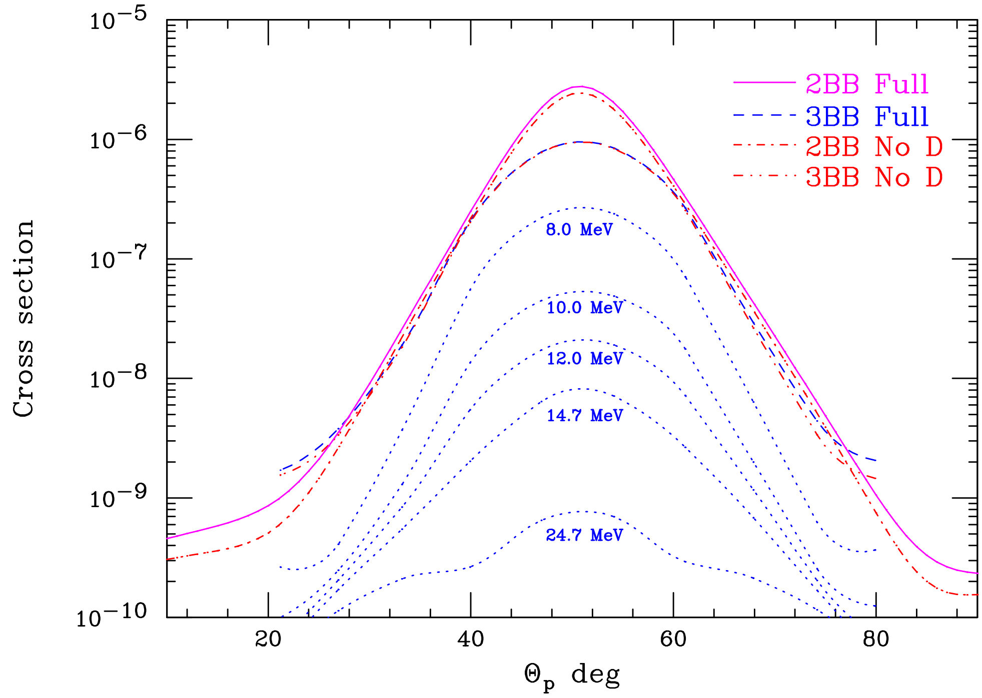

Figure 2: Calculated $^3\vec{\mathrm{He}}(\vec{\mathrm{e}}, \mathrm{e}'\mathrm{p})$–cross sections as a function of the scattering angle of the knocked out proton for kinematics K1. The dotted lines are the calculated result for selected E_m–values as labeled in the figure.

Also shown in figure 2 is the 3BB contribution integrated over the E_m–range from threshold to 24.7 MeV (dash) compared to the 2BB cross section (solid). The dot–dash and the dot–dot–dash lines indicate calculations where the D–state contribution of the ^{3}He–ground state has been turned off. As expected, a significant effect of the D–state is only observed for the extreme wings of the Fermi cone.

As discussed in section 1, the sensitivity to the D–state can be significantly enhanced with measurements of the asymmetries. This is quantitatively discussed in the following via a comparison of the asymmetries for various calculated results; the result of a full calculation, a symmetrized plane wave impulse approximation (PWIAS), and a calculation for which the D–state contribution in the ground state wave function has been turned off. Results will be discussed for the extreme kinematics K1 and K3. For clarity results for the intermediate kinematics K2 are not discussed. All results have been averaged over the E_m–range considered.

Figure 3 summarizes the results of A_x and A_z for the $^3\vec{He}(\vec{e}, e'n)$–reaction for kinematics K1 (top of the quasi–elastic peak) and for kinematics K3 (low ω–side of the quasi–elastic peak) as a function of the knocked out neutron scattering angle. The corresponding $\vec{q}$–angles are 50.5^o and 57.5^o for K1 and K3 respectively. The results where the D-state contribution to the ^{3}He–ground state wave function is turned off is indicated with the dash line. In addition, the results for the PWIAS result (dash–dot) is shown.

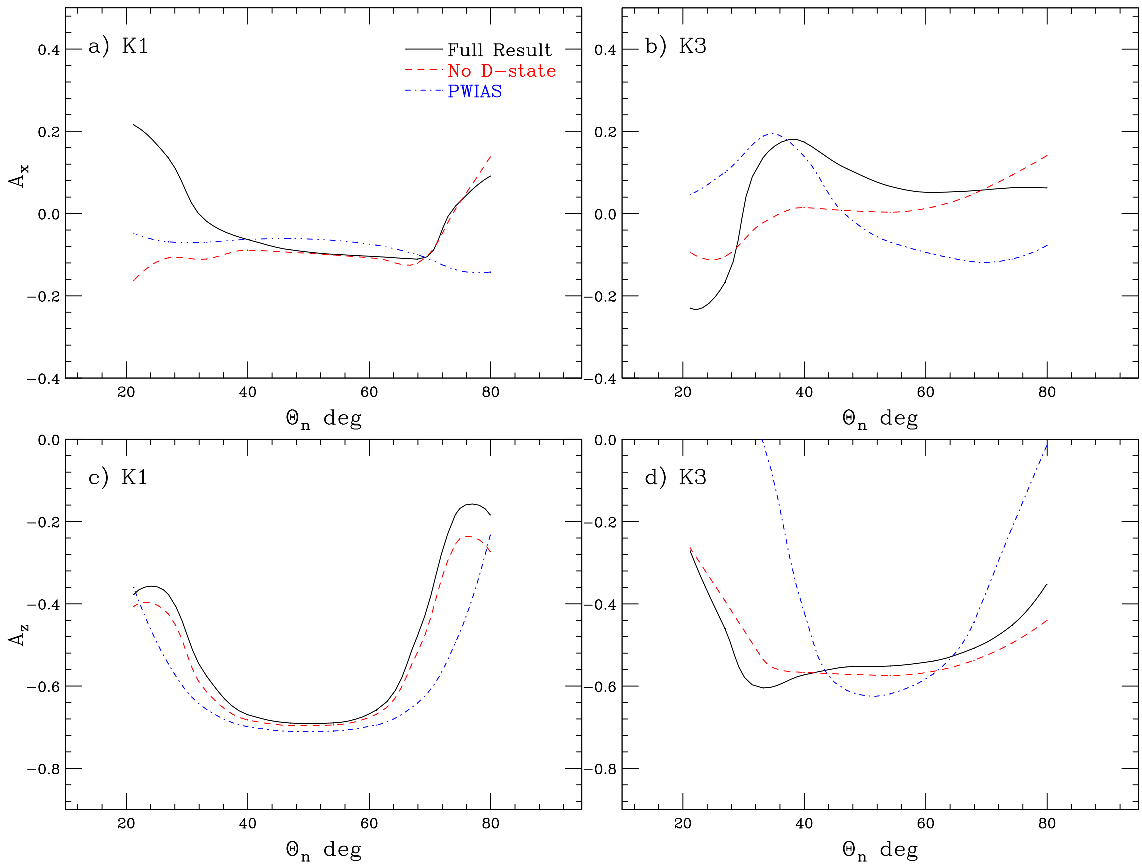

Figure 3: Calculated results of asymmetries for the $^3\vec{He}(\vec{e}, e'n)$–reaction as a function of the neutron angle. In a) and b) the asymmetry perpendicular to $\vec{q}$, A_x, and in c) and d) parallel to $\vec{q}$, A_z, is shown.

For kinematics K1 the results confirm the well known expectations for a measurement of the neutron form factors. In the direction of $\vec{q}$ one finds almost no effect of the D-state in both A_x and A_z. Except for the effect of FSI, the calculated results are close to the results using the expression for a free polarized neutron target [37] and a dipole and Galster parameterization for G_{mn} and G_{en} respectively [38]. In the wings of the Fermi cone some D–state effects are predicted, but also significant effects due to FSI. This is also particularly the case for kinematics K3 where FSI are dominant over most of the angular range.

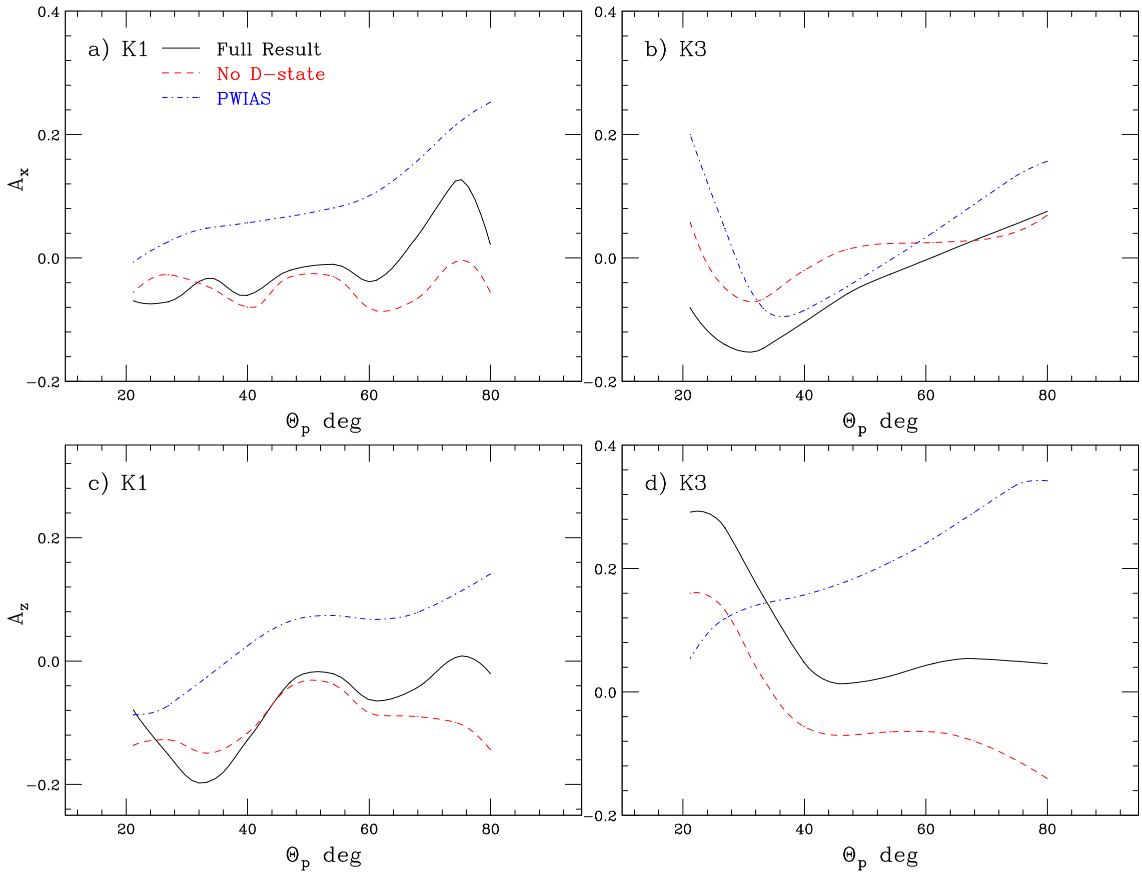

Figure 4: Calculated results of asymmetries for the $^3\vec{\mathrm{He}}(\vec{e}, e'p)$–reaction as a function of the proton angle. In a) and b) the asymmetry perpendicular to $\vec{q}$, A_x, and in c) and d) parallel to $\vec{q}$, A_z, is shown.

Figure 4 shows the analog results for the $^3\vec{\mathrm{He}}(\vec{e}, e'p)$–reaction. Whereas FSI–contributions are significant over most of the kinematical range studied, they do not mask the particularly large signal of the D–state for kinematics K3. In particular for A_z the D-state does not only affect the wings of the Fermi cone but has a large effect also in the direction of $\vec{q}$. Thus, the full Faddeev calculation preserves the effect which was studied by Blankleider via the simple PWIA–calculation. However, FSI–effects have to be studied as well.

A clean signal for FSI–effects can be found for kinematics K1 in the direction of $\vec{q}$ for $^3\vec{\mathrm{He}}(\vec{e}, e'p)$ provided the 2BB– and the 3BB–channel can be separated. In figure 5 we show for kinematics K1 the separate contribution of the 2BB– and the 3BB–channel for A_x. The asymmetry for the 2BB–channel does not show a large effect of FSI. However, a very large FSI signal is observed for the 3BB–channel, leading to a large asymmetry. In addition, for both channels, very little dependence on the small wave function components is observed. The large asymmetry in the 3BB suggests that the remaining two–nucleon system is left with a high probability in a $^1S_0$–state. In this case the spin of the knocked out proton is strongly correlated with the spin of the neutron which, for low Fermi momentum, is always parallel to the nuclear spin. Thus, the strong FSI effect simulates an almost 100% polarized proton target.

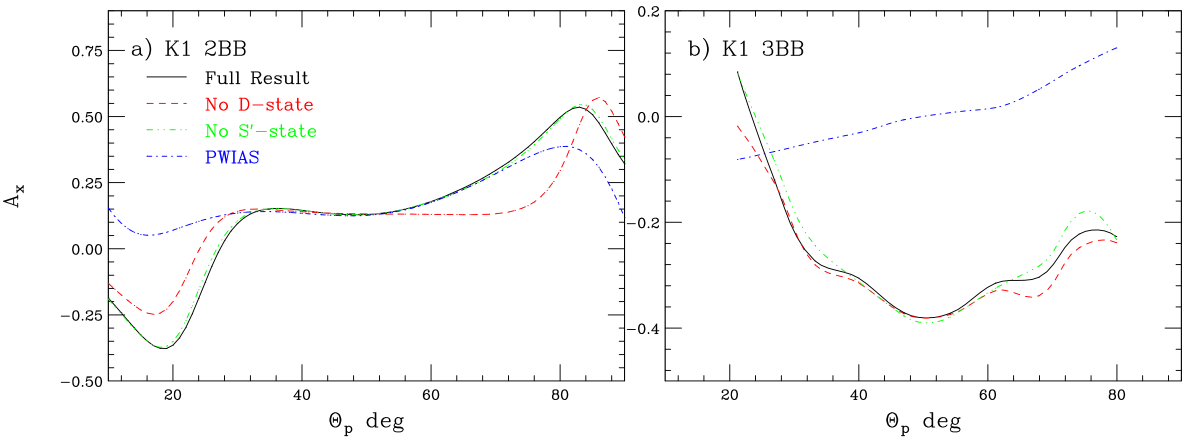

Figure 5: Results of A_x for the 2BB–channel (left) and the 3BB–channel (right) in the reaction $^3\vec{\mathrm{He}}(\vec{\mathrm{e}},\mathrm{e'p})$ for kinematics K1.

Contrary to the simple calculations of the past, in particular to the calculations by Blankleider and Woloshyn [13], Schulze and Sauer [31], and Nagorny and Turchinetz [39] the present results do not indicate any large effects of the S'–state for the observables and the kinematic range studied. All the listed calculations predicted a sizeable effect of the S'–state for the asymmetry in $^3\vec{\mathrm{He}}(\vec{\mathrm{e}},\mathrm{e'p})$–scattering close to the quasi–elastic peak.

In summary, the results of the calculations indicate appropriate windows to separate the effects of the small D–state and of FSI. In addition, the absorption mechanism of the photon by one and two–body currents can be studied and the various existing nucleon–nucleon force models with consistently added currents can be probed.

A measurement of A_x and A_z for both the $^3\vec{\mathrm{He}}(\vec{\mathrm{e}},\mathrm{e'p})$ and the $^3\vec{\mathrm{He}}(\vec{\mathrm{e}},\mathrm{e'n})$ reaction over a large kinematic range will improve significantly our knowledge of the D–state contribution to the ground state of ^{3}He. No significant effect of the very small contribution of the S'–state has been found.

The measurement of A_x and A_z at the quasi-elastic peak with a clean separation of the 2-body and 3-body contributions to the proton asymmetry will test the predicted large signal of FSI and will provide a clean test of the correctness of the present calculations. The use of spectrometer B, placed in the direction of $\vec{q}$, will allow for the required separation.

One should note that with the planned setup of the experiment we will cover the kinematical range of K1–K3 and study *simultaneously* the $^3\vec{\mathrm{He}}(\vec{\mathrm{e}},\mathrm{e'n})$ and the $^3\vec{\mathrm{He}}(\vec{\mathrm{e}},\mathrm{e'p})$–reaction over a significant range of the Fermi cone and the $^3\vec{\mathrm{He}}(\vec{\mathrm{e}},\mathrm{e'p})$–reaction along $\vec{q}$ with the ability to separate the 2BB– and 3BB–channel. The realization of the setup will be described in sec. 3.

2.2 Previous Experiments

2.2.1 The G_{en} experiments at MAMI

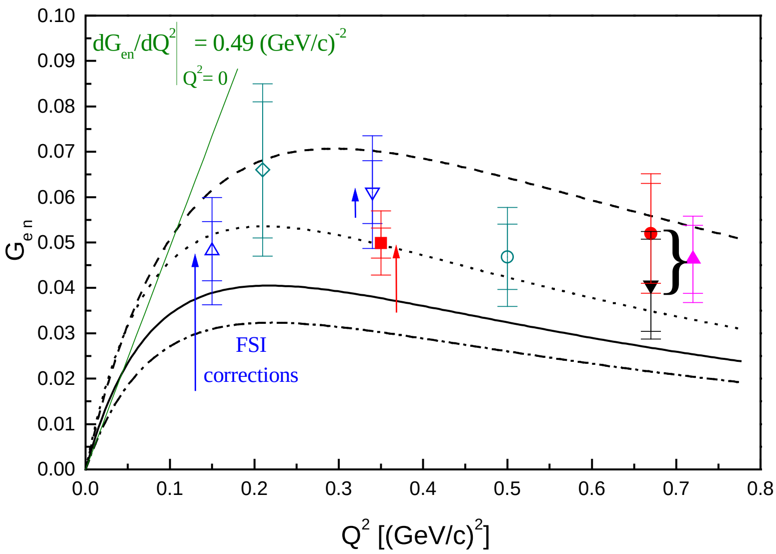

Figure 6: G_{en} extracted from quasi-elastic scattering of polarized electrons from ^{2}H and $^3\vec{\mathrm{He}}$. The data are taken from refs. [20–25]. The lines are fits to the elastic deuteron results [40] for the NN–potentials Nijmegen (dashed), Argonne V14 (dots), Paris (solid) and Reid–Soft–Core (dot–dashed).

An increased interest in the neutron electric form factor G_{en} has triggered a series of experiments at MAMI in Mainz exploiting the expertise in polarized electron source and polarized target techniques, followed by experiments at NIKHEF and JLab. Apart from the interest in this fundamental property of the neutron by itself, G_{en} serves as a benchmark for tests of nucleon models and as input for parity violation experiments. Exploiting polarization observables overcome the problem arised in elastic scattering off the deuteron, where the extraction of G_{en} depends on the NN potential chosen. The double polarization experiments constitute a great breakthrough as they measure the ratio of G_{en}/G_{mn} and due to the precise knowledge of G_{mn} determine G_{en} absolutely.

However, at low Q^2 there are sizeable corrections for FSI and MEC effects to be considered. The corrected results for several G_{en} analysis [20–25] are given in Fig. 6. In addition, the arrows indicate the size of corrections which have to be applied. One clearly notices their diminishing size for increasing Q^2. Whereas the corrections for the deuteron are in general believed to be well under control as these calculations have been tested by several other experimental observables, the situation is less favorable for ^{3}He. The calculations by the Bochum group for ^{3}He including FSI and MEC have been available only recently. They have been applied first [32] to the G_{en} –measurement at Q^2=0.35 (GeV/c)^2 by Becker *et al.* [23]. The predictions constitutes over 30% correction to the data; at the highest data points [25, 41] this reduces to a ≈10%.

There is a clear need for further tests of these calculations to be performed best at different kinematical situations.

2.2.2 The $^3\vec{\mathrm{He}}(\vec{\mathrm{e}},\mathrm{e}'\mathrm{p})$ and $^3\vec{\mathrm{He}}(\vec{\mathrm{e}},\mathrm{e}'\mathrm{n})$ experiments at NIKHEF

Recently asymmetries A_z and A_y^o have been measured at NIKHEF for the exclusive $^3\vec{\mathrm{He}}(\vec{\mathrm{e}},\mathrm{e}'\mathrm{p})$ and $^3\vec{\mathrm{He}}(\vec{\mathrm{e}},\mathrm{e}'\mathrm{n})$ reactions [26]. The experiments have been performed at the internal target facility of the AMPS stretcher at low momentum transfer of Q^2=0.16 (GeV/c)^2. An electron beam polarization of 60% was reached and the ^{3}He was polarized through optical pumping to about 50%. The scattered electrons were momentum analyzed by the BigBite spectrometer in coincidence with the ejected nucleons, where a range telescope had been used for protons and a TOF detection system for the neutrons. The 2BB– and 3BB–breakup channel could not be separated in this experiment; therefore the cross sections have been added for the region –10< E_m <12 MeV.

The data on the induced asymmetry A_y^o and the longitudinal spin asymmetry A_z have been compared to model calculations by Golak [32], Nagorny [39] and Laget [42] respectively. A value of A_y^o=-0.50±0.05 has been obtained for the $^3\vec{\mathrm{He}}(\vec{\mathrm{e}},\mathrm{e}'\mathrm{n})$-reaction, while A_z=0.21±0.09 for $^3\vec{\mathrm{He}}(\vec{\mathrm{e}},\mathrm{e}'\mathrm{p})$ and A_z=–0.56±0.18 has been measured for the $^3\vec{\mathrm{He}}(\vec{\mathrm{e}},\mathrm{e}'\mathrm{n})$-reaction [26]. Within errors the data are in agreement with the predictions by Golak. The calculations indicate that final state interactions play an important role at the low momentum transfer of Q^2=0.16 (GeV/c)^2. No conclusion could be drawn about the internal structure of ^{3}He or the energy dependence of FSI or MEC effects.

2.2.3 The unpolarized ^{3}He(e,e′p) experiment at MAMI

In the Q^2-range of the proposed investigation, an unpolarized ^{3}He(e,e′p) experiment has been performed at the three spectrometer facility of MAMI with the aim to separate the longitudinal and transversal response functions [6, 7]. Data have been taken at three different momentum transfers extending the measurements to high missing energies (E_m <150 MeV) and high missing momenta (p_m <300 MeV/c). An energy resolution of $\Delta E_m \leq$0.5 MeV has been obtained, which enabled a clear separation of the two- and three-body breakup channels as demonstrated for E_e=855 MeV in Fig. 7 [7]. The data are shown with and without radiative corrections. The different procedures produced comparable results at the low missing energies. One notices that no strength is left for missing energies higher than 20 MeV. The momentum distributions have been extracted for the three settings which correspond to the values of photon polarization ε=0.21, 0.46 and 0.65. For the two-body breakup channel the three momentum distributions (Fig. 8, left) agree very well with each other. At low p_m they are lower than the previous data by Jans *et al.* [43]. Using the CC1 prescription by deForest it was concluded that the experimental ratio L/T is slightly

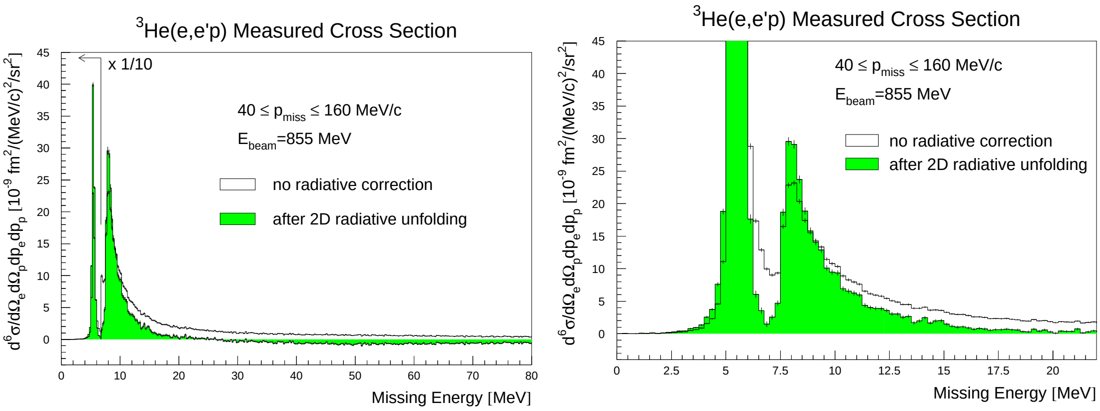

Figure 7: Missing energy spectrum for the $^3\vec{\mathrm{He}}(\vec{e},e'p)$ reaction for the full range (left) and the relevant range up to E_m <20 MeV (right) taken from [7]. The data are shown before and after the radiative tail corrections.

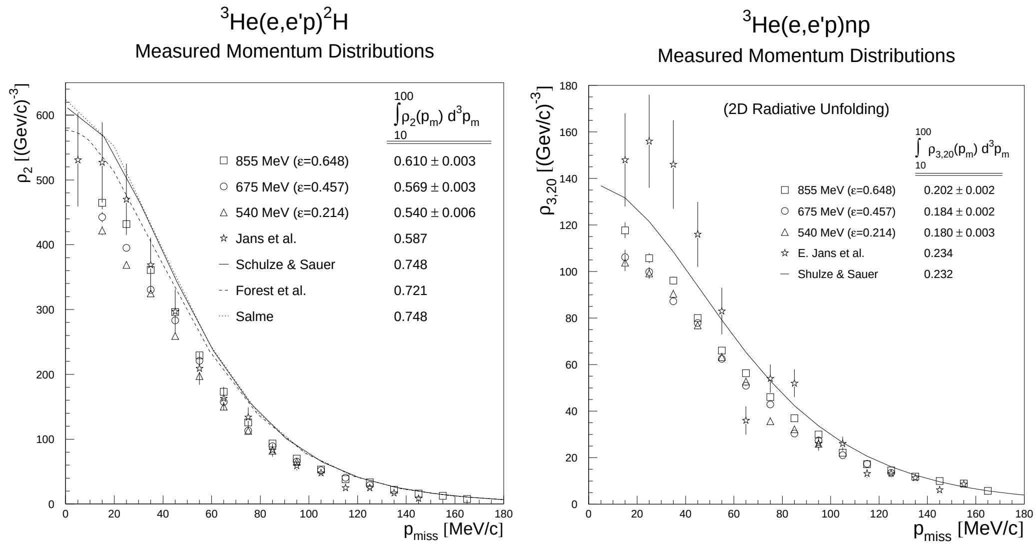

Figure 8: Missing momentum distributions for the $^3\vec{\mathrm{He}}(\vec{e},e'p)^2\mathrm{H}$ (left) and the $^3\vec{\mathrm{He}}(\vec{e},e'p)np$ (right) reactions as measured by Florizone *et al.* [7].

larger than predicted. Good agreement and similar conclusions were reached for the three-body breakup channel ^{3}He(e,e$'$p)np as demonstrated in the right panel of Fig. 8.

These data show that the two breakup channels can be separated easily even with slightly worse energy resolution. The variation of the momentum distributions with the photon polarization is too small for any separation of the response functions.

3 Proposed Experiment

3.1 Kinematics and Layout

We propose to measure the asymmetries A_x and A_z in the exclusive reactions $^3\vec{\rm He}(\vec{\rm e},{\rm e}'{\rm p})$ and $^3\vec{\rm He}(\vec{\rm e},{\rm e}'{\rm n})$ at $Q^2 = 0.32$ (GeV/c^2), where relativistic effects are small and where the non-relativistic calculations of Golak et al. (s. 2.1) are reliable. The calculations use an electron energy of 790 MeV and therefore we will use this kinematics in the following. But one should note that similar kinematics using the nominal electron energy of 855 MeV at MAMI would not change the main features and conclusions of the proposed experiment. The kinematics is given in table 1. The outgoing electron is scattered under 48^o into spectrometer A with a momentum

Q^2 (GeV/c^2)	q MeV/c	E MeV	E′ MeV	θ_e deg	θ_q deg
0.32	600	790	585–715	48	50

Table 1: Kinematics (rounded values)

acceptance of 20 % and a solid angle of 28 msr (see fig. 9). Protons and neutrons are detected simultaneously over a large angular range from 24^o to 40^o and 60^o to 76^o using two identical nucleon detectors, each with a solid angle of of 77 msr (s. sec. 3.3 for details). This covers the tails of the Fermi cone, where the $L \neq 0$ components of ^{3}He are putting their strongest fingerprint to the measured quantity, the asymmetry. Further, this arrangement allows us to examine the responses symmetric to $\vec{q}$. The nucleon detectors will be located at 32^o and 68^o respectively on a separate stand. In addition to the two nucleon detectors protons are detected in the direction of $\vec{q}$ with spectrometer B (momentum acceptance: 15 %, solid angle: 5.6 msr), which allows the separation of 3-body and 2-body breakup of ^{3}He due to the good momentum resolution of 10^{-4}. Using this setup a wide kinematical range is covered and the three kinematics K1– K3, for which in sec. 2.1 the calculation of Golak et al. were presented, are measured simultaneously.

The resolution reached in the experiment with spectrometer B will be limited mainly due to multiple scattering and energy straggling at the 1.5 mm thick glass walls of the target cell. Between target and collimator of each spectrometer an opening in the target shielding box minimizes the material in the path of the reaction products. From the experience of a previous experiment [6], it is known that a resolution in the missing energy spectrum of order 0.5 MeV for $^3{\rm He}({\rm e},{\rm e}'{\rm p})$ can be achieved. Given a factor of three for the thickness of target and windows in the present proposal, we expect to reach a resolution of 1.5 MeV in missing energy which will be sufficient for the separation of 2-and 3-body breakup. For further details about the spectrometers see [44].

Both, the target region and the nucleon detector is well shielded with lead to reduce the background rates. In addition, each of the nucleon detectors has a lead collimator with an opening towards the target.

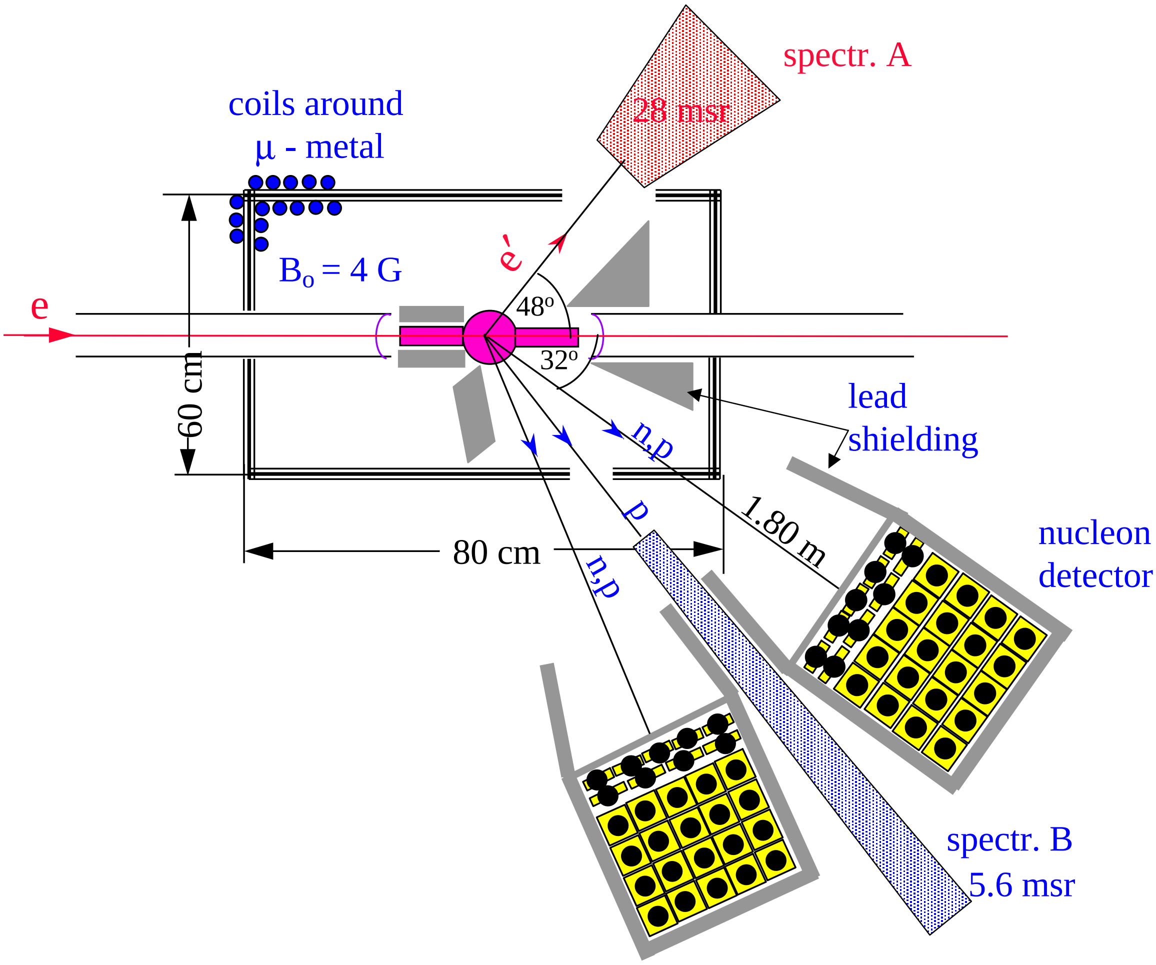

Figure 9: Setup of the proposed experiment in the spectrometer hall at MAMI.

3.2 Beam and Target

Due to the progress of the polarized electron source at MAMI over the last years, a polarized electron beam of 20 μA and a polarization of 80 % is routinely produced from InGaP- or GaAsP-cathodes [45, 46]. For the experiment the standard beam line of the spectrometer hall is used and the electron polarization will be measured with the Møller polarimeter [47] which is based on the same principle as the one described in [48]. Beam polarization measurements with an accuracy of less than 2 % in a time of the order of 5 min. are possible.

Only a small modification of the beam line is necessary close to the target. In front of the target an additional beam spot monitor is installed to check the beam alignment at the target small windows, which are 1 cm in diameter. Because the polarized ^{3}He–target is not directly connected to the beam line, the upstream and downstream vacuum tube is sealed off separately by 20 μm beryllium foils.

The ^{3}He–cell is placed in a homogeneous magnetic field of about 4 Gauss. The spin of the ^{3}He–nuclei can be rotated in all directions via rotation of the magnetic

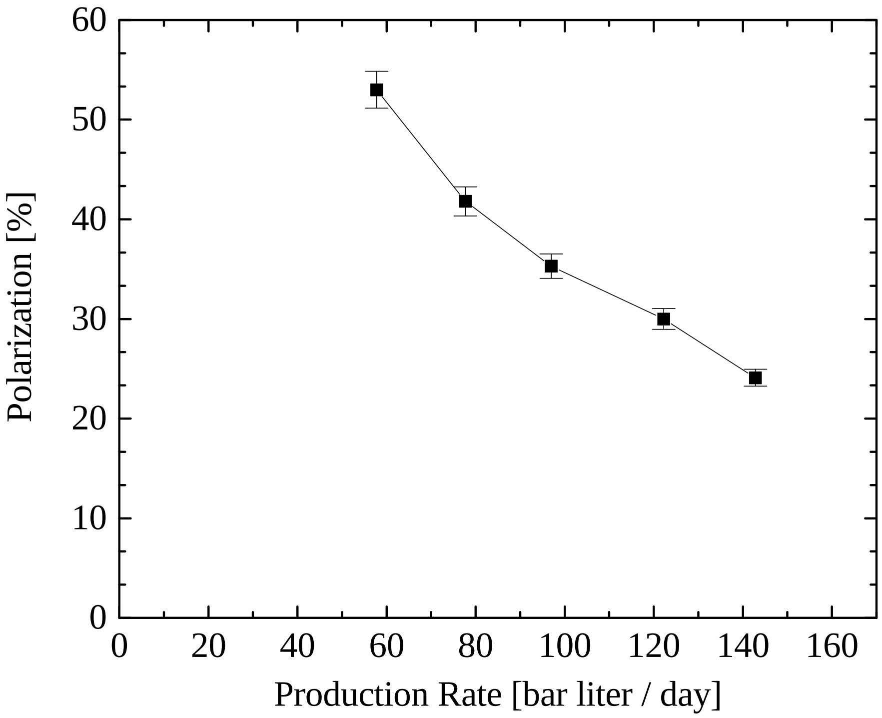

Figure 10: Polarization versus production rate of polarized ^{3}He

holding field . This allows measurements with the target spin parallel or perpendicular to the direction of the momentum transfer as well as measurements where the target spin is aligned perpendicular to the scattering plane.

The size of the cell is adapted to the needs of the experiment. Its total length is 20 cm and entrance and exit windows made out of 20 μm thin copper foil which can withstand a pressure difference of 8 bar (tested). The central part of the quartz cell is spherical (diameter: 9 cm) with an extension (quartz tube of 5 cm) on two opposite sides. The volume of the inner sphere is $\approx$350 cm^3, which is 96% of the total gas volume.

The ^{3}He gas is spin-polarized by direct optical pumping in its metastable (1s2s $^3S_1$) state at pressures around 1 mbar [49, 50]. In order to reach the high densities required for these experiments, the polarized gas is compressed into a target cell by means of a non-magnetic titanium piston compressor. Once the desired pressure in the range of 3 to 8 bar is reached, the cell is disconnected from the ^{3}He polarizer- and compressor unit and transported to the target chamber in the spectrometer hall. A homogeneous magnetic field of a few Gauss is necessary to guide the spins. Polarization losses during compression are negligible. Thus, the degree of ^{3}He polarization in the low pressure optical pumping cells is the same as in the target cells. Fig. 10 shows the measured polarization as a function of the production rate. At a flux of about 3 bar·liter per hour, a nuclear spin polarization of ^{3}He of 50% is achieved.

Long relaxation times are a prerequisite for a remote type of operation. The target cells are made of quartz glass. The inner walls are coated with cesium in order to reduce polarization losses due to wall relaxation. Indeed, in cesium-coated cells a total relaxation time of $T_1 = 276$ hours has been observed at a gas pressure of 1.4 bar [51]. Under these conditions wall relaxation is no longer the dominant relaxation mechanism. Dipolar coupling between ^{3}He spins limits the storage time with regard to higher pressures with $T_{1,dipolar}$ [h] = 750/p [bar].

The situation is different if the polarized gas is exposed to a charged particle beam. Scattered electrons create paramagnetic centers in the glass which lead to an enhanced wall relaxation. Consequently, under electron beam conditions the total relaxation time drops to 30 - 40 hours. Therefore, the transportable target cells must be changed twice a day, so that a high average polarization is maintained. Typically, over a 12 hour period an average polarization of $P_{av} = 38$ % prevails. It takes about 1 hour to change the cell and to replace it by a freshly polarized one.

Polarization measurements will be accomplished by two means. During the experiment, the polarization will be monitored by NMR techniques. This technique applies a pulsed, resonant r.f field which tilts the magnetization out of the z-axis by an angle $\alpha < 1^o$. The signal amplitude yields a relative measurement of the nuclear polarization only, but allows to monitor the decay of the polarization (relaxation) with high precision. In order to obtain an absolute value of P, we use the technique of adiabatic fast passage (AFP) to flip the magnetic moment of the sample by 180^o. The polarization losses during one AFP-flip are less than 0.2%. By means of a flux gate magnetometer positioned close to the sphere (central part of the target cell), the relative change of the magnetic field can be detected. Since the field distribution outside a homogeneously magnetized sphere is that of a magnetic dipole, the polarization of the gas can be measured with a relative precision of $\Delta P/P$ = 1 - 3% [52].

3.3 Detectors

One of the nucleon detectors was already successfully implemented during the G_{en} experiment at MAMI [53]. The second one will be identical to allow for a symmetric arrangement. Each of the detectors contains four layers of five BC400 plastic scintillator bars of dimensions 50 x 10 x 10 cm^3. This results in a solid angle of 77 msr at a distance from the target of 180 cm. Due to the fivefold segmentation the scattering angle can be binned easily into bins of the size $\Delta\theta = 3.2^o$. Photo multipliers are mounted on each side of the bar for reconstruction of the out–of–plane angle. A measured resolution of 2.6 mrad was obtained using 50 MeV protons [54]. This segmentation will allow the study of the angular dependence of the asymmetry. The discrimination between neutrons and protons relies on two layers of plastic ΔE detectors preceeding the bars. In the previous G_{en}–experiment an neutron efficency of ≈ 25 % was determined [41].

The entire detector is shielded with 10 cm lead except for the opening towards the target, where the shielding is reduced to 2 cm. This thinner shielding avoids unnecessary absorption of nucleons and it has a small conversion probability due to charge exchange reactions (e.g. (e,e'p)+(p,n)), but provides moderate rates in the nucleon detector even at smaller angles as it was shown by previous experiments [24, 55] in the same or similar environments.

3.4 Rates and Beamtime Request

		(e,e'n)		(e,e'p)			
				2BB+3BB		2BB	3BB
	$\theta_{n,p}$	32^o	68^o	32^o	68^o	50^o	50^o
K1	[nb/MeV/sr^2]	0.09	0.13	0.33	0.7	28	7
	[Hz]	0.019	0.027	0.55	1.18	17.6	4.4
K2	[nb/MeV/sr^2]	0.01	0.11	0.07	0.6	1.25	0.75
	[Hz]	0.0021	0.023	0.117	1.00	0.78	0.47
K3	[nb/MeV/sr^2]	0.001	0.017	0.02	0.13	0.1	0.05
	[Hz]	$2.1\,10^{-4}$	0.0036	0.033	0.22	0.06	0.03

Table 2: Cross sections and rates for the three kinematics and various reactions(see text).

The cross sections in table 2 for $^3\vec{\mathrm{He}}(\vec{\mathrm{e}},\mathrm{e'n})$ and $^3\vec{\mathrm{He}}(\vec{\mathrm{e}},\mathrm{e'p})$ are taken from the full Faddeev calculation by Golak et al. at the central angles of both nucleon detectors and spectrometer B. For the latter we distinguish between 2BB and 3BB. The cross sections are integrated over the E_m–range from threshold to 24.7 MeV. They depend on the outgoing nucleon angle in a mostly linear way (except at the top of the quasi-elastic peak) and therefore it is sufficient for the count–rate estimate to take the values at the central angles. Therefore each nucleon detector is binned into 5 bins of 15 msr, which provides 5 data points of A_x and A_z at each kinematics. For spectrometer A and B the nominal solid angles of 28 msr and 5.6 msr respectively and a momentum acceptance of 20 % for spectrometer A is assumed. At a central momentum of 650 MeV/c this corresponds to an ω–acceptance of $\approx$ 120 MeV, over which the three kinematics K1, K2, K3 are roughly equal spread (see fig. 1). Therefore bins of 40 MeV in the energy transfer $\Delta\omega$ are used. The effective target length acceptance of the spectrometer at the chosen angle is 6 cm. A beam current of 10 μA and a target pressure of 5 bar results in a luminosity of 50 (nb sec)$^{-1}$. A detector efficiency based on the measured value [41] of 25 % for neutrons is taken.

The count rates are shown in table 2. The comparably small solid angle of 5.6 msr of spectrometer B is largely compensated by the increased cross section at the top of the quasi-elastic peak. In addition, the asymmetry for the 3-body breakup in $(e, e'p)$ is quite large (s. fig. 5). On the other hand, the count rates for kinematics K3 are very small, because it is far from the top of the quasi-elastic peak and corresponds to high missing momenta.

In the following, the statistical error of the asymmetry reached in the proposed experiment will be estimated. An electron beam of 10 μA and 80 % polarization is assumed. With the experience from the recent G_{en} experiment [25] an average target polarization of 35 % is a conservative value. For 200 h pure data taking the expected statistical uncertainties of the asymmetry for each kinematics and reaction is shown in table 3. Note, that the amount of beam time has to be doubled to reach the same statistics for each asymmetry A_x and A_z. However, all three kinematics and reactions shown in table 2 are measured simultaneously.

	(e,e'n)		(e,e'p)			
			2BB+3BB		2BB	3BB
$\theta_{n,p}$	32^o	68^o	32^o	68^o	50^o	50^o
K1	0.03	0.026	$5.7\,10^{-3}$	$3.9\,10^{-3}$	$1.0\,10^{-3}$	$2.0\,10^{-3}$
K2	0.09	0.028	0.012	$4.2\,10^{-3}$	$4.8\,10^{-3}$	$6.1\,10^{-3}$
K3	0.29	0.07	0.023	$9.0\,10^{-3}$	0.017	0.024

Table 3: . Estimated statistical uncertainty of the asymmetry for 200 h data taking.

The errors are lower or around 0.01 except for the $(e, e'n)$–reaction in kinematics K3. For the $(e, e'p)$–reaction in kinematics K3 this has to be compared to a sizeable D-state effect of the order of 0.1 in both asymmetries (see Fig. 4b) and d)). The small rates for kinematics K3 do not prevent to achieve the goals of the proposal. Further, as described in section 2.1 kinematics K1 is the most interesting one for the $(e, e'p)$–reaction using spectrometer B, where 2BB and 3BB can be separated. For the 3BB an error bar of 0.002 has to be compared to an FSI–effect of the order of 0.3.

In light of the previous G_{en} measurements [23, 32], a significant test of the full Faddeev calculations is possible with the $(e, e'n)$ measurements in kinematics K1. Less significant tests are possible for kinematics K2 and K3. However, in order to test a predicted largely absent D–state effect for $(e, e'n)$ in kinematics K3 the five data points for each nucleon detector can be combined to improve the statistical accuracy.

The setup of the experiment is quite elaborate as it includes the installation of two nucleon detectors and the polarized ^{3}He–target. From the experience with the G_{en}–experiment, which used the same setup, but only one nucleon detector, we estimate a setup time of 400 h. To test the setup we will need 80 h beam before data taking can start. During this time checkout of detectors, electronics and data acquisition for this non-standard setup will be performed. In addition, data using ^{2}H in a similar kind of target cell will be taken for calibration purposes. The proposed uncertainties in table 3 are reached in 400 h of data taking, 200 h for each asymmetry. Because of the relaxation of the polarization in the ^{3}He–target 2 h per day are needed to change the target cell twice a day, which guarantees a polarization of 35 % in average. Therefore we estimate an overhead of 30 % to the requested beam time in total, which sums up to 520 h.

References

[1] A. Kievsky, M. Viviani, S. Rosati, D. Hübner, W. Glöckle, H. Kamada, H. Witala, and J. Golak. *Phys. Rev.*, C58:3085, 1998.

[2] W. Glöckle et al. Electronuclear Physics with Internal Targets and the BLAST Detector, edited by R. Alarcon and R.G. Milner. *World Scientific*, Cambridge:185, 1999.

[3] R. Schiavilla, V.G.J. Stoks, W. Glöckle, H. Kamada, A. Nogga, J. Carlson, R. Machleidt, V. R. Pandharipande, R. B. Wiringa, A. Kievsky, S. Rosati, and M. Viviani. *Phys. Rev.*, C58:1263, 1998.

[4] A. Amroun et al. *Nucl. Phys.*, A579:596, 1994.

[5] J.M. LeGoff et al. *Phys. Rev.*, C55:1600, 1997.

[6] R.E.J. Florizone et al. *Phys. Rev. Lett.*, 83:2308, 1999.

[7] R.E.J. Florizone. *The Longitudinal and Transverse Response of the (e,e'p) Reaction in Helium–3 and Helium–4 in the Quasielastic Region.* PhD thesis, MIT, 1999.

[8] W. Glöckle, H. Witala, D. Hüber, H. Kamada, and J. Golak. *Phys. Rep.*, 274:107, 1996.

[9] I. Sick. *Lecture Notes in Physics, Springer*, 260:42, 1986.

[10] J. Jourdan et al. *Nucl. Phys.*, A453:220, 1986.

[11] H. Anklin et al. *Nucl. Phys. A*, 636:189, 1998.

[12] M. Ericson and N. Lo Judice. *Nucl. Phys. A*, 475:199, 1987.

[13] B. Blankleider and R.M. Woloshyn. *Phys. Rev. C*, 29:538, 1984.

[14] D. Leinweber, T. Draper, and R.M. Woloshyn. *Phys. Rev.*, D46:3067, 1992.

[15] Aron M. Bernstein and Barry R. Holstein (Eds.). Proceedings of the workshop On Chiral Dynamics Cambridge, USA 25-29 July 1994, Springer Lecture Notes in Physics, 1994.

[16] B. Krusche et al. *Phys. Rev. Lett.*, 74:3736, 1995.

[17] P. Hoffman-Rothe et al. *Phys. Rev. Lett.*, 78:4697, 1997.

[18] V. Hejny et al. *Eur. Phys. J.*, A6:83, 1999.

[19] W. Xu et al. *Phys. Rev. Lett.*, 85:2900, 2000.

[20] I. Passchier et al. *Phys. Rev. Lett.*, 82:4988, 1999.

[21] C. Herberg et al. *Eur. Phys. J*, A5:131, 1999.

[22] M Ostrick et al. *Phys. Rev. Lett.*, 83:276, 1999.

[23] J. Becker et al. *Eur. Phys. J.*, A6:329, 1999.

[24] D. Rohe et al. *Phys. Rev. Lett.*, 83:4257, 1999.

[25] J. Bermuth. PhD thesis, University of Mainz, 2001.

[26] H.R. Poolman. *Quasifree Spin–dependent Electron Scattering from a Polarized ^{3}He Internal Target.* PhD thesis, Vrije Universiteit,, 1999.

[27] J. Arends et al. MAMI–Proposal A2/1-97, 1997.

[28] Z.E. Meziani et al. JLab Proposal PR 94–010, 1994.

[29] C. Ciofi degli Atti, S. Scopetta, E. Pace, and G. Salme. *Phys. Rev. C*, 48:968, 1993.

[30] C. Ciofi degli Atti and S. Scopetta. *Phys. Lett. B*, 404:223, 1997.

[31] R.W. Schulze and P.U. Sauer. *Phys. Rev.*, C48:38, 1993.

[32] J. Golak, G. Ziemer, H. Kamada, H. Witala, and W. Glöckle. *Preprint*, nucl-th/0008008, 2000.

[33] J. Golak. privat communication, 2000.

[34] K.A. Dow et al. *Phys. Rev. Lett.*, 61:1706, 1988.

[35] D. Day et al. *Ann. Rev. Nucl. Part. Sci.*, 40:357, 1990.

[36] A.S. Raskin and T.W. Donnelly. *Ann. Phys.*, 191:78, 1989.

[37] R.G.Arnold, C.E. Carlson, and F.Gross. *Phys. Rev. C*, 21:1426, 1980.

[38] S. Galster, H. Klein, J. Moritz, K.H. Schmidt, D. Wegener, and J. Bleckwenn. *Nucl. Phys.*, B32:221, 1971.

[39] S.I. Nagorny and W. Turchinetz. *Phys. Lett.*, B429:222, 1998.

[40] S. Platchkov et al. *Nucl.Phys.*, A510:740, 1990.

[41] D. Rohe. PhD thesis, University of Mainz, 1998.

[42] J.M. Laget. *Phys. Lett.*, B276:398, 1992.

[43] E. Jans et al. *Nucl. Phys.*, A475:687, 1987.

[44] K.I. Blomqvist et al. *Nucl. Instr. and Methods*, A403:263, 1998.

[45] K. Aulenbacher et al. Proceedings PST, International workshop on polarized Sources and Targets, Erlangen, p288-292, 1999.

[46] K. Aulenbacher et al. private communication, 2000.

[47] P. Bartsch. PhD thesis, University of Mainz, 2001.

[48] M. Hauger et al. *Nucl. Instr. Meth. A*, in print, 1999.

[49] F.D. Colgrove et al. *PR*, 132:2561, 1963.

[50] G. Eckert et al. *Nucl. Instr. and Meth.*, A320:53, 1992.

[51] W. Heil. private communication, 1995.

[52] E. Wilms et al. *Nucl. Instr. and Meth.*, A320:491, 1992.

[53] W. Heil. Measurements of the electric form factor of the neutron. MAMI–Proposal of the A1–collaboration, 1995.

[54] M. Hauger. private communication, 2000.

[55] H. Anklin et al. *Phys. Lett.*, B336:313, 1994.